

# Irradiation induced doping of topological insulators, route to surface controlled electronic transport

Marcin Konczykowski  
Laboratoire des Solides Irradiés  
Ecole Polytechnique  
Palaiseau, France



In collaboration with Lukas Zhao, Haiming Deng, Inna Korzhovska, Milan Begliarbekov, Zhiyi Chen, Lia Krusin-Elbaum (CUNY, New York)

Evangelos Papalazarou, Marino Marsi (LPS, Orsay)

Luca Perfetti, (LSI, Palaiseau)

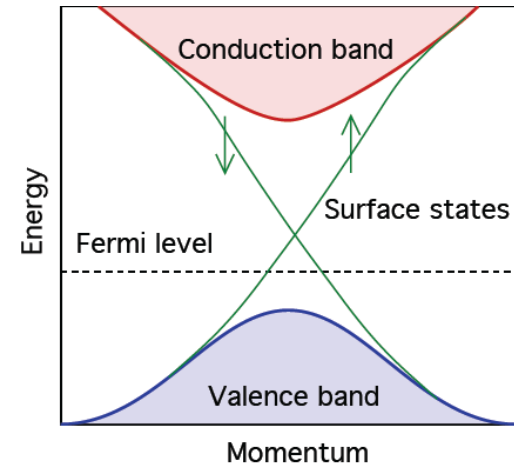
Andrzej Hruban, Agnieszka Wołos (Institute of Physics, Warsaw)

Support from ANR-NSF project “IRIDOTI”

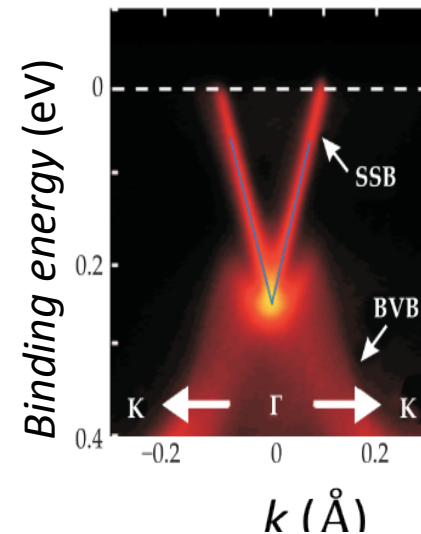
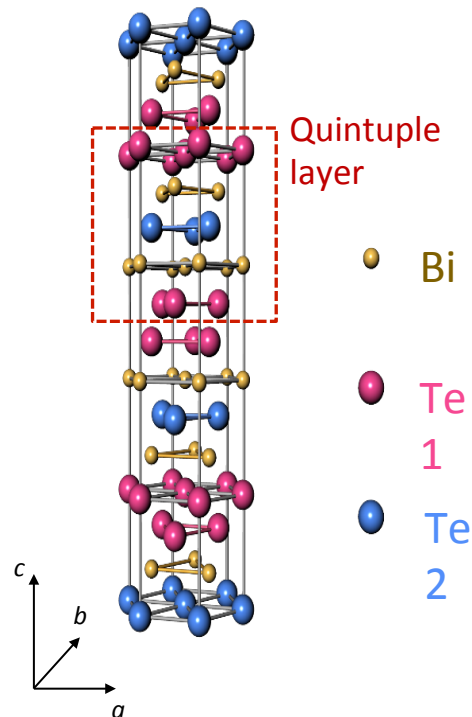


# 3D Topological insulators

- $A_2B_3$  family ( $Bi_2Te_3$ ,  $Bi_2Se_3$ )
- Share the same rhombohedral crystal structure
- $A_2B_3$  were first predicted to be TIs using first principle calculation
- Should have a single Dirac cone on the surface  
(Shou-Cheng Zhang & Zhong Fu, Nat Phys 5, 438 (2009))



- ✓ Confirmed by ARPES  
(Xia, et. al. Nat Phys 2009;  
Hsieh, et. al. Science 2009;  
Chen, et. al. Science 2009)
- ✓ Spin-resolved ARPES  
detected left-handed  
helical spin texture of the  
massless Dirac fermions  
and the absence of  
backscattering from non-  
magnetic impurities (Xia,  
et. al. Nat Phys 2009; Hsieh, et.  
al. Science 2009)



Science 325, 178 (2009).

# Critical problem for applications

Charged defects provide free carriers in volume and high conduction deny access to surface states in electronic transport.

## This work:

Counteracting bulk disorder

→ developed new technique using heavy ion and electron irradiation

(1) Native defects

(2) Controlled introduction of out-of-equilibrium vacancies

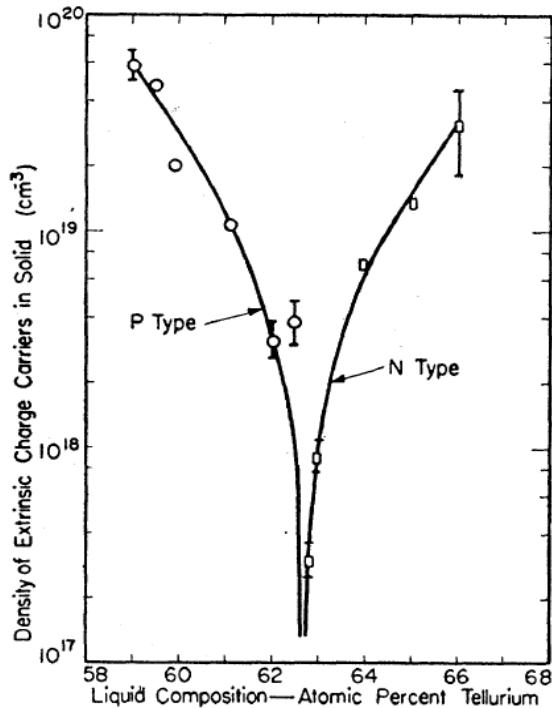
(3) Irradiation induced metal – insulator transition

(4) Application to  $\text{Bi}_2\text{Te}_3$  and  $\text{Bi}_2\text{Se}_3$

(5) Observation of electronic transport via surface states

(6) Next steps: gated devices, magnetically doped TI, crystalline TI's

# Native defects in $\text{Bi}_2\text{Te}_3$ and $\text{Bi}_2\text{Se}_3$



Composition dependence of conductivity in  $\text{Bi}_2\text{Te}_3$   
C.B Satterthwaite & R.W. Ure,  
Phys. Rev. 108, 1164 (1957)  
Simple picture:  
Cation (Bi) vacancy – donor  
Anion (Te) vacancy - acceptor

Present status: more complex native defects

- Double charged donor Te or Se vacancies
- Antisite defects Se on Bi place acting as acceptors
- Antisite Bi on Se or Te as multiple charged donor.

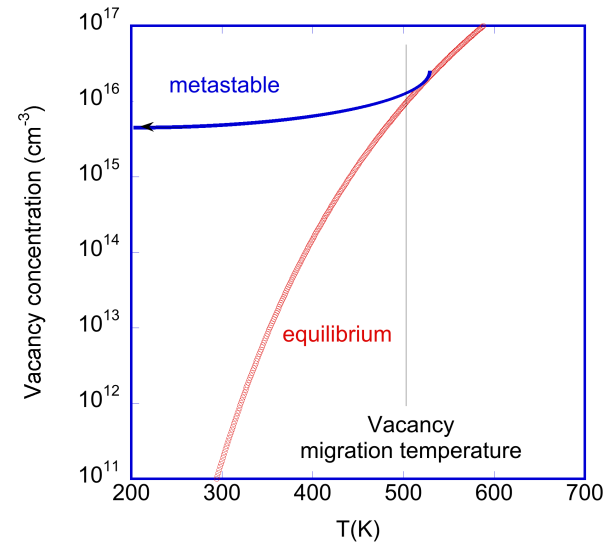
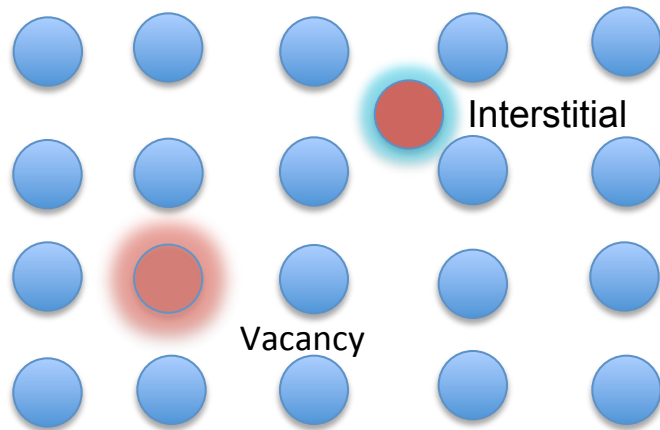
Lack of consensus: mostly theoretical calculation in DFT

For review see:

“Controlling Bulk Conductivity in Topological Insulators: Key Role of Anti-Site Defects” *D. O. Scanlon et al. Adv. Mater.*, **24**, 2154, (2012)

# Native defects : vacancies & interstitials

Energies involved:	Formation energy	Migration energy
Vacancy	1.3 eV	0.7 eV (Cu)
Interstitial	2-3 eV	0.03-0.05 eV



Crystal growth:

Defects concentration “frozen” at temperature determined by migration energy. Significant metastable concentration of vacancies, negligible of interstitials (lower migration energy)

Method to change defects concentration: quench or energetic particle electron irradiation.

# Low temperature electron irradiation facility SIRIUS operated by LSI at Ecole Polytechnique



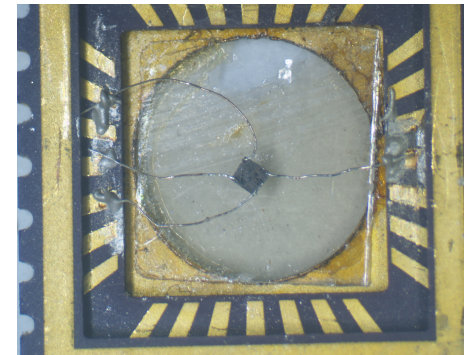
NEC Pelltron electron  
accelerator 0.3-2.5 MeV



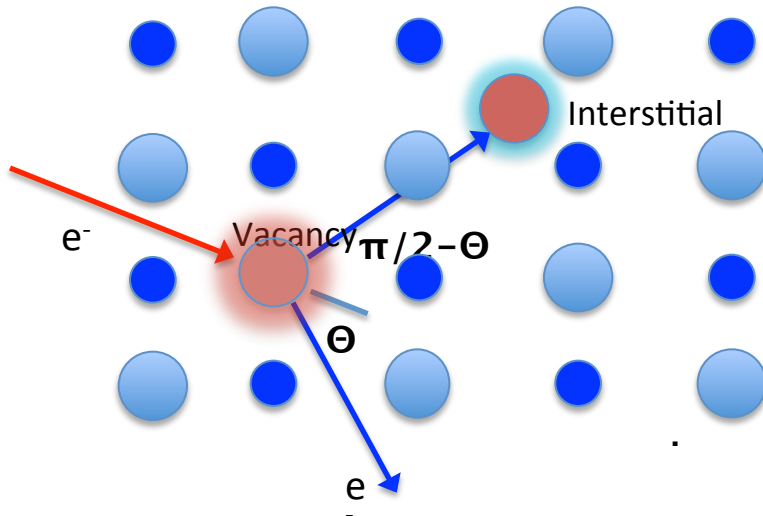
H<sub>2</sub> condenser on GM cryocooler  
Useful cooling power >25W at 20K  
Possible high doses >10C/cm<sup>2</sup>

$$N_d = \sigma \varphi \quad (\varphi \text{ particles per unit area})$$

Ba(FeAs<sub>0.55</sub>P<sub>0.45</sub>)<sub>2</sub> crystal mounted on chip  
holder with bore for electron irradiation and  
easy transfer to VTI cryostat



# Frenkel pairs generated by electron irradiation

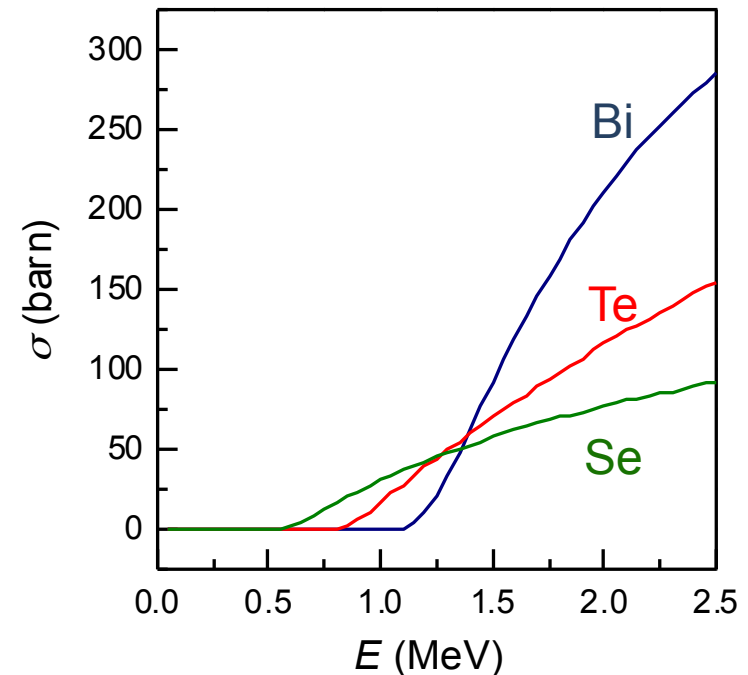


Rutherford collision of relativistic electron of energy  $E$  with nucleus of mass  $M$  at angle  $\Theta$ :  $E = E_m \sin^2(\Theta)/2$ .

Cross section for defect creation defined by empirical parameter: energy threshold to eject atom from its site  $E_d$

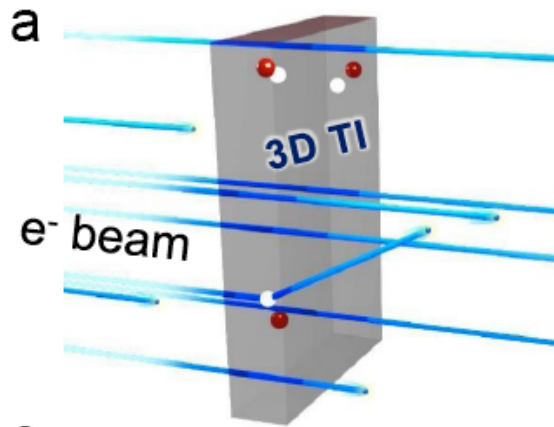
$$\sigma = \frac{2\pi}{E_m} \int_{E_d}^{E_m} \frac{d\sigma(E)}{d\Theta} P_d(E) dE$$

Defect creation rate in bi-atomic compound estimated by SECTE software (D. Lesueur, F. Beneu, Ph. Bois)



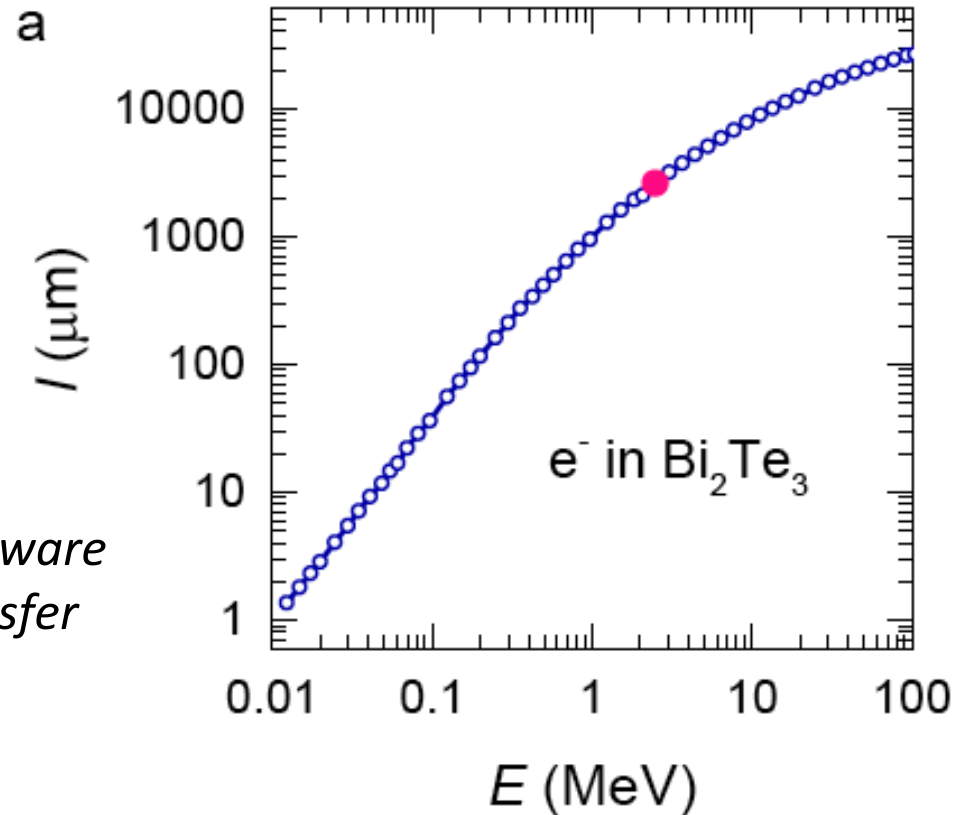
At energy far above threshold, defects on heavy Bi sublattice outnumber those on Te or Se

# Penetration range of 2.5 MeV electrons in $\text{Bi}_2\text{Te}_3$



Stopping power simulations: ESTAR software (NIST) with two channels of energy transfer from electron projectile to crystal:

- Electronic excitations
- Rutherford collisions (dominant)

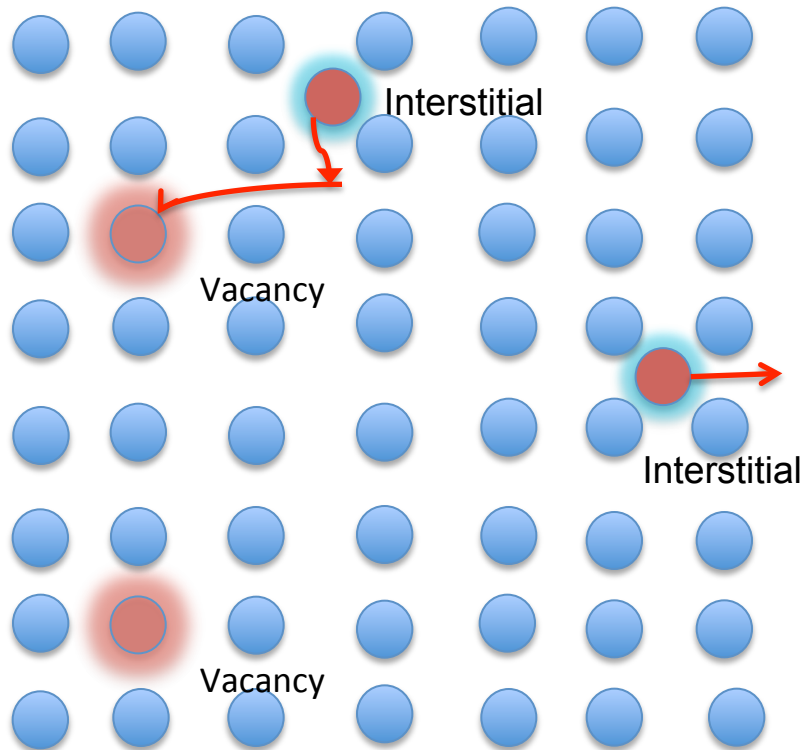


Penetration range above 2mm guarantees uniform defect creation in typically 20 $\mu\text{m}$  thick samples.



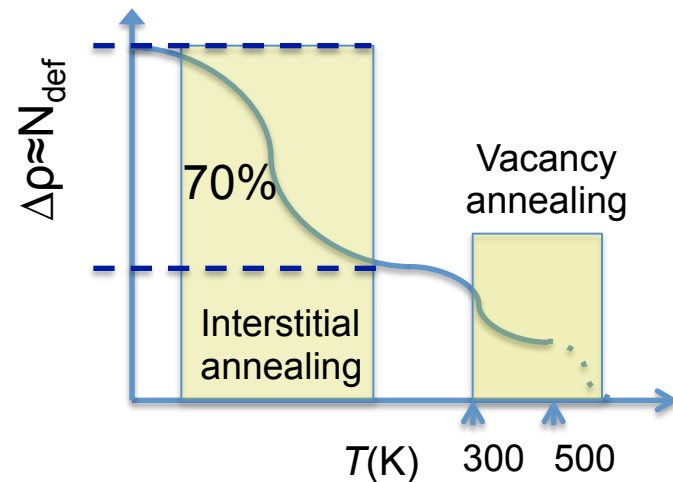
# Low temperature electron irradiation

Irradiation at low temperature prevents defect migration and agglomeration



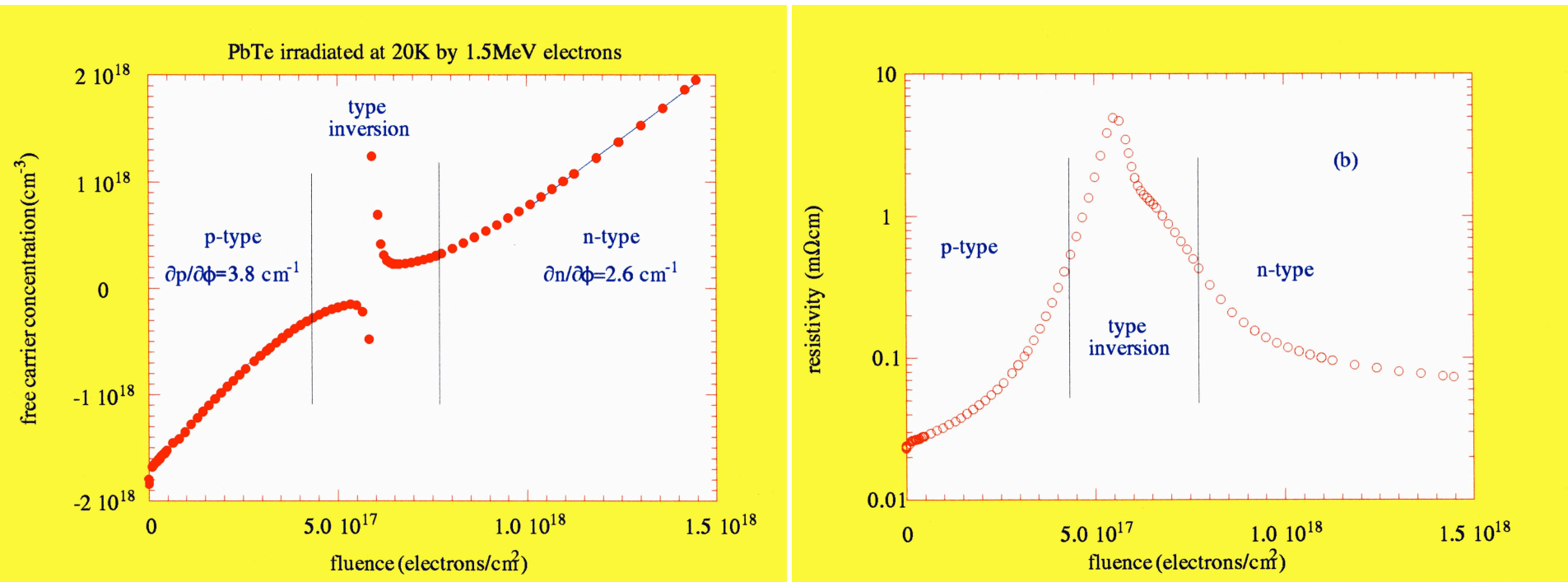
Low temperature irradiation followed by warming to room temperature results in vacancy type disorder

Creation of uniform spread of Frenkel pairs. On warming, interstitial become mobile (80-120K), those close to the vacancy recombine, while the interstitials from distant pairs migrate to remote sinks (eg. surface) leaving stable vacancies.



# Low temperature electron irradiation: semiconductors

Realisation: in situ measurement of Hall effect and resistivity during irradiation of p-type PbTe crystals with 1.5 MeV electrons at 20K



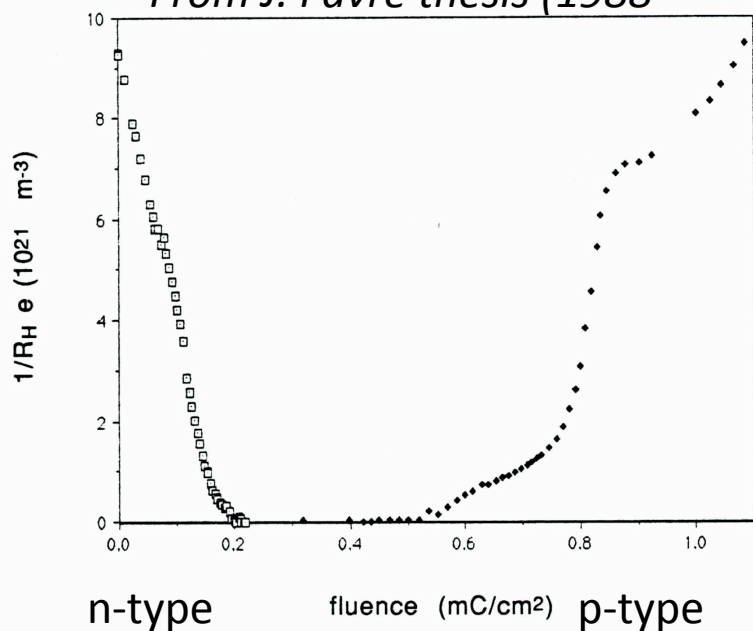
Cumulative effect of irradiation induced vacancies & interstitials: n-type doping of PbTe. Starting from p-type material smooth upward shift of Fermi level until neutrality point. Change of slope of concentration vs. dose: indication of crossing of defect level. Close to neutrality point: extreme compensation  $10^{-6}$

# Doping effect of irradiation induced defects

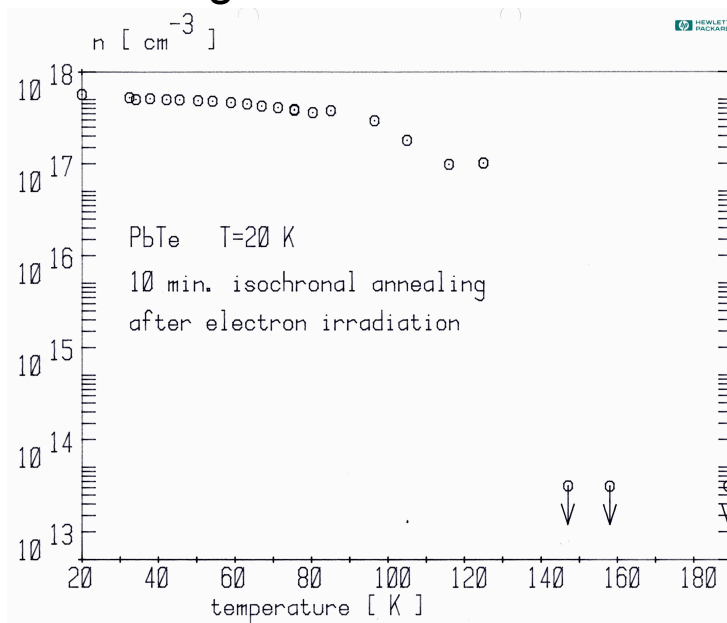
Phenomenology: donor type doping in IV-VI and II-VI semiconductors, acceptor type doping in most of III-V InSb, GaAs).

Example, evolution of Hall constant during irradiation with 2 MeV electrons

*From J. Favre thesis (1988)*

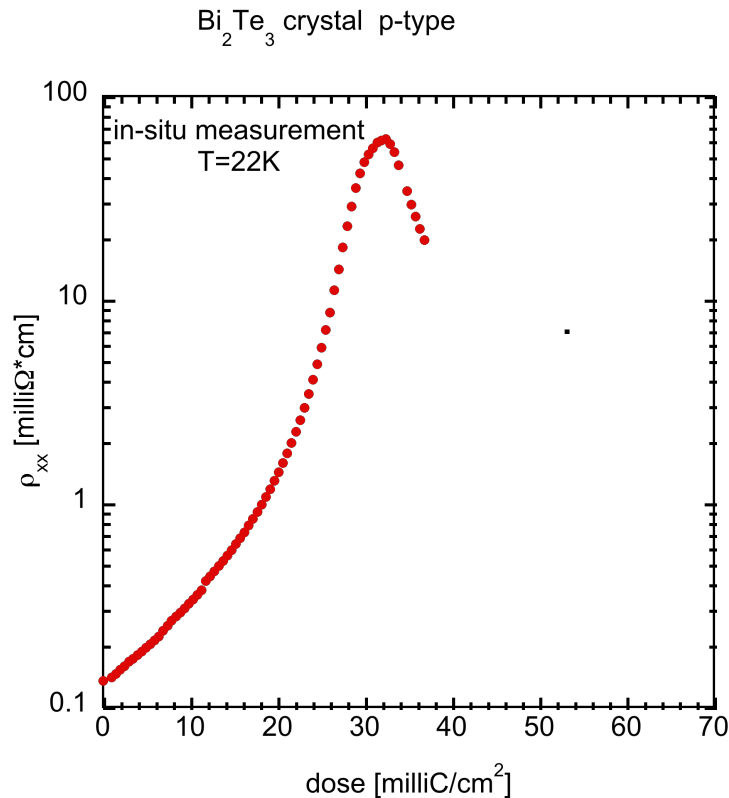


Complex behaviour: donor type doping during low temperature irradiation (cumulative action of vacancies and interstitials) turning to acceptor action of vacancies left after annealing of interstitials.



Ultimately low carrier concentrations ( $<10^{13} cm^{-3}$ ) obtained in PbTe by irradiation followed by annealing  
Uniform and precise doping controlled on  $<10^{12} cm^{-3}$  level

# Conductivity type inversion by irradiation with 2.5 MeV electrons of $\text{Bi}_2\text{Te}_3$ and $\text{Bi}_2\text{Se}_3:\text{Ca}$



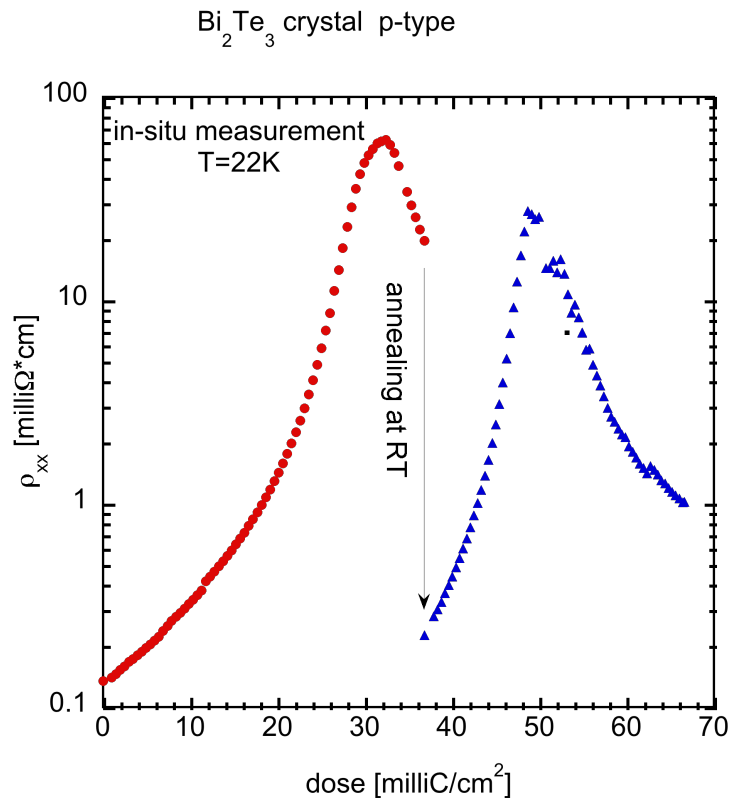
In situ measurement at liquid hydrogen (20-22K) in the function of irradiation dose.

Maximum of  $\rho_{xx}$  marks the crossing of neutrality point.

What happens if we warm up to room temperature?

*Starting from p-type material with hole concentration  $4 \cdot 10^{18} \text{ cm}^{-3}$  resistivity increases donor type doping*

# Conductivity type inversion by irradiation with 2.5 MeV electrons of $\text{Bi}_2\text{Te}_3$ and $\text{Bi}_2\text{Se}_3:\text{Ca}$



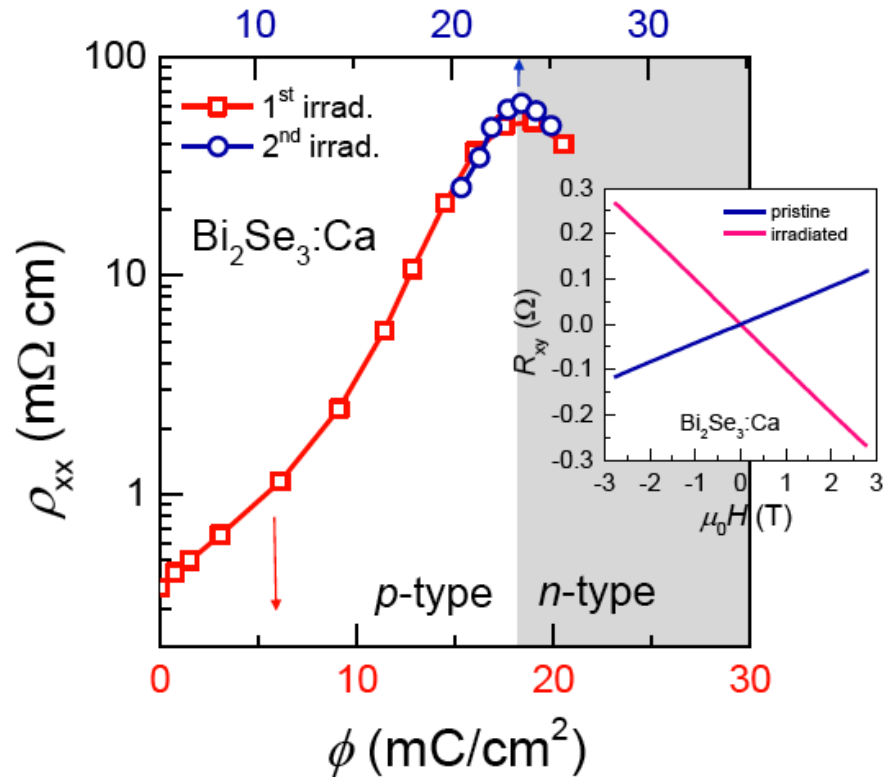
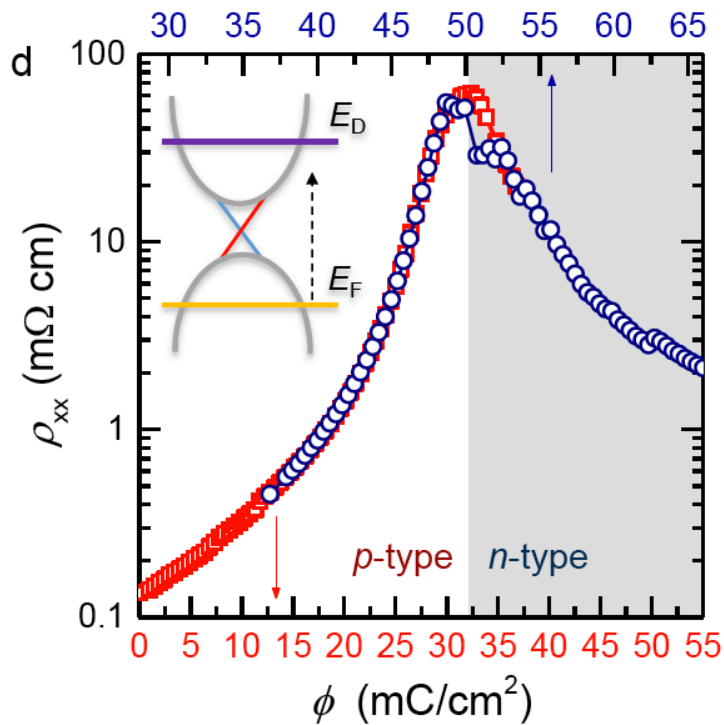
In situ measurement at liquid hydrogen (20-22K) in the function of irradiation dose.

Maximum of  $\rho_{xx}$  marks the crossing of neutrality point.

What happens if we warm up to room temperature?

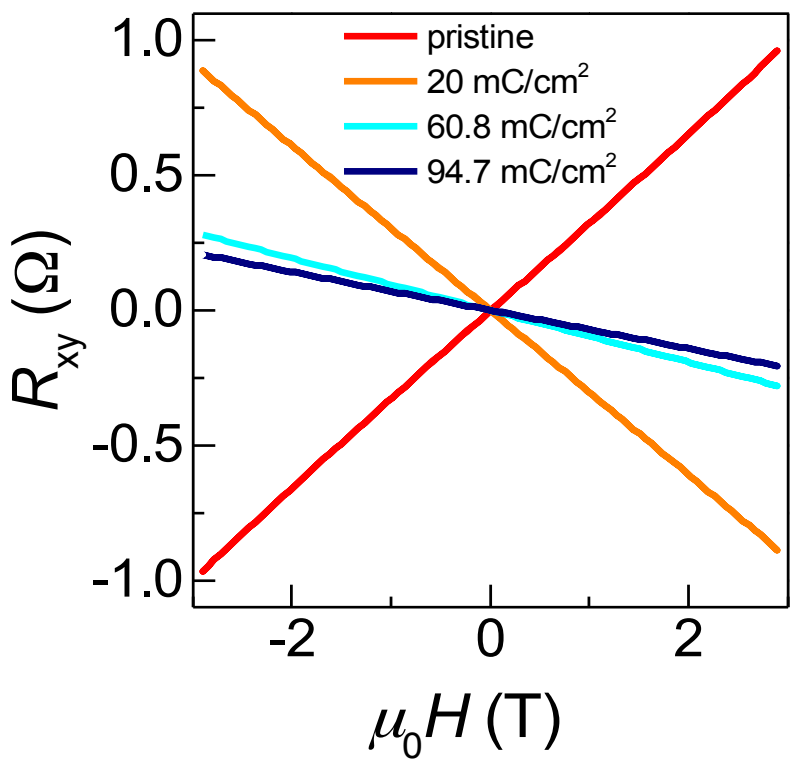
70% of damage lost due to partial annealing. Return to p-type but one can restart the process.

# Conductivity type inversion by irradiation with 2.5 MeV electrons in $\text{Bi}_2\text{Te}_3$ and $\text{Bi}_2\text{Se}_3$

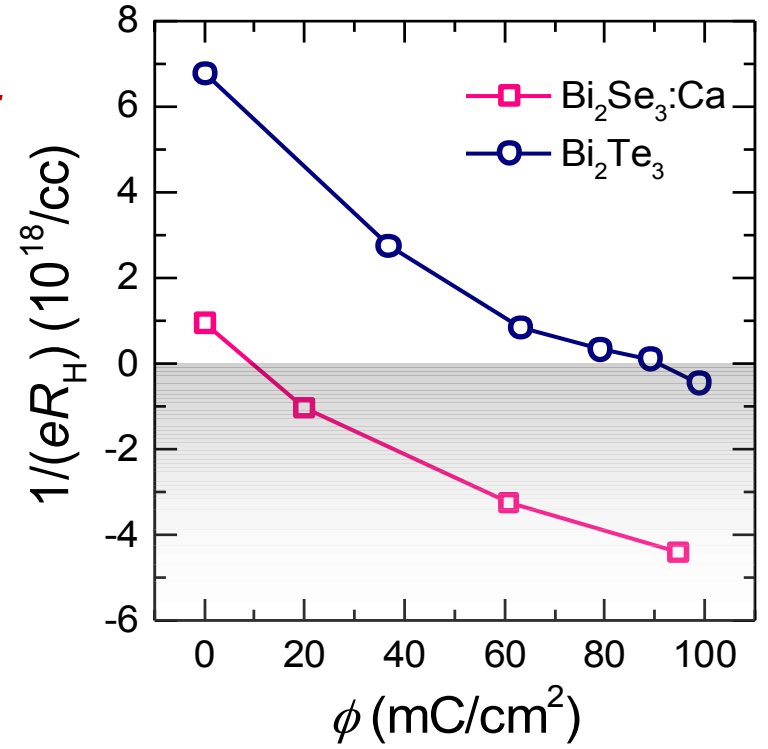


The same scenario in  $\text{Bi}_2\text{Te}_3$  and  $\text{Bi}_2\text{Se}_3$ : 2-3 orders of magnitude increase of resistivity before reaching maximum marking conductivity type inversion. Warming to room temperature results in partial annealing.

# Effect of 2.5 MeV electron irradiation on p-type $\text{Bi}_2\text{Te}_3$

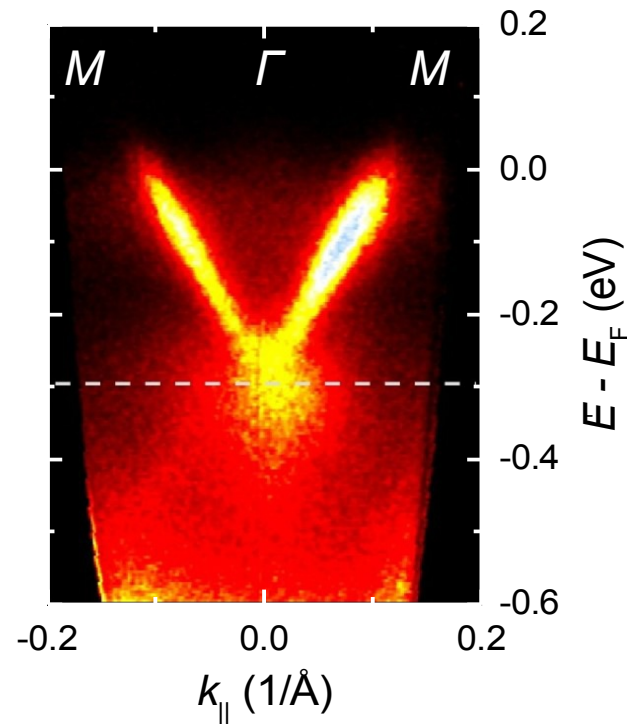


$\text{Bi}_2\text{Te}_3$  Hall resistance measured at 4.2K after different doses of irradiation



Very similar rates of carrier concentration vs. dose variation in  $\text{Bi}_2\text{Te}_3$  and  $\text{Bi}_2\text{Se}_3$ .  
Indication that defects on Bi sites are relevant.

# ARPES of 2.5 MeV electron irradiation p-type $\text{Bi}_2\text{Te}_3$



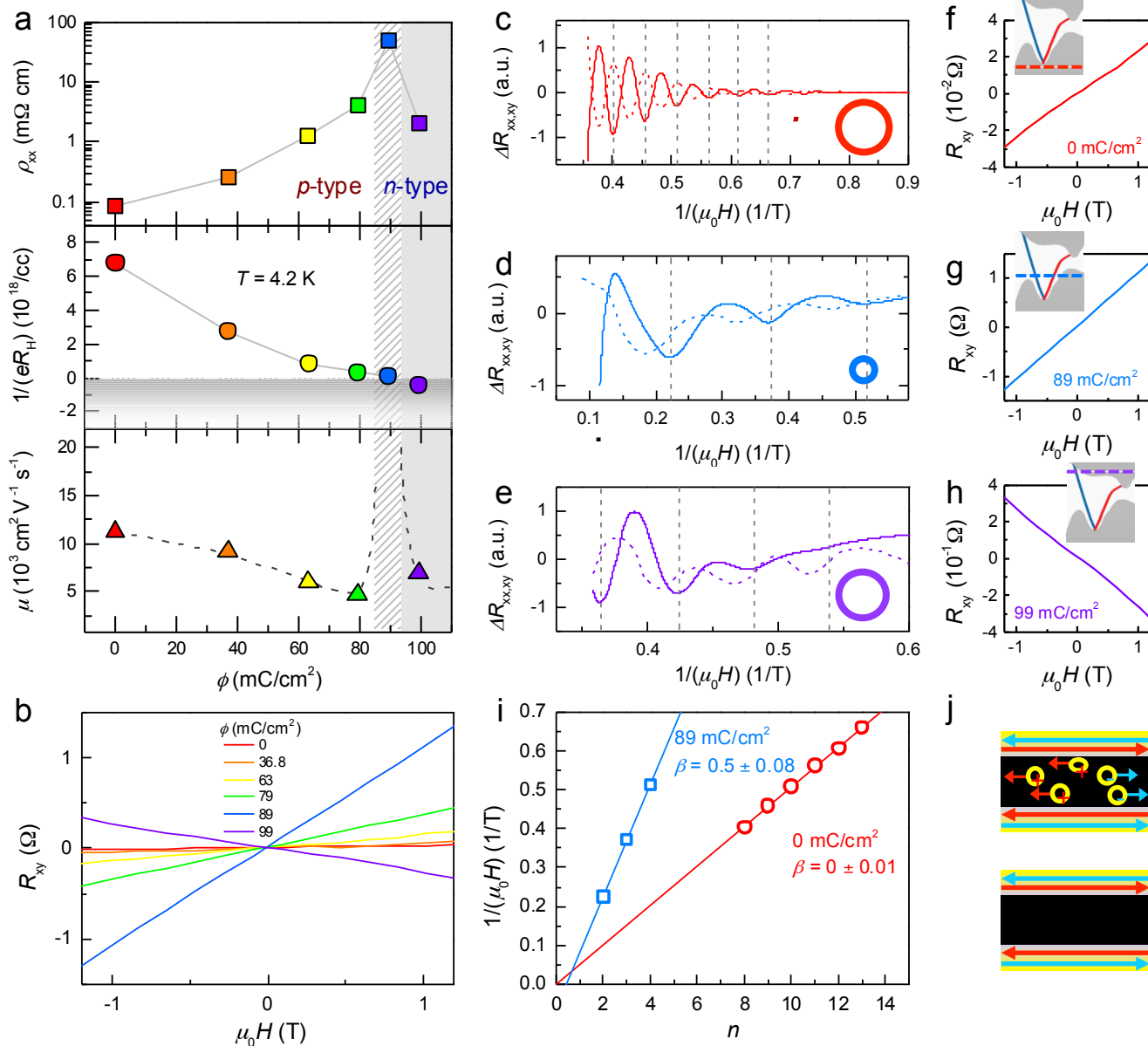
Example of a laser ARPES spectrum for a  $\text{Bi}_2\text{Te}_3$  crystal irradiated to the dose of  $1.7 \text{ C/cm}^2$ .

Effect of irradiation is to move Fermi energy to the edge of the conduction band consistent with  $n$ -type conduction.

**Dirac cones unaffected by disorder**



# Effect of 2.5 MeV electron irradiation on p-type $\text{Bi}_2\text{Te}_3$

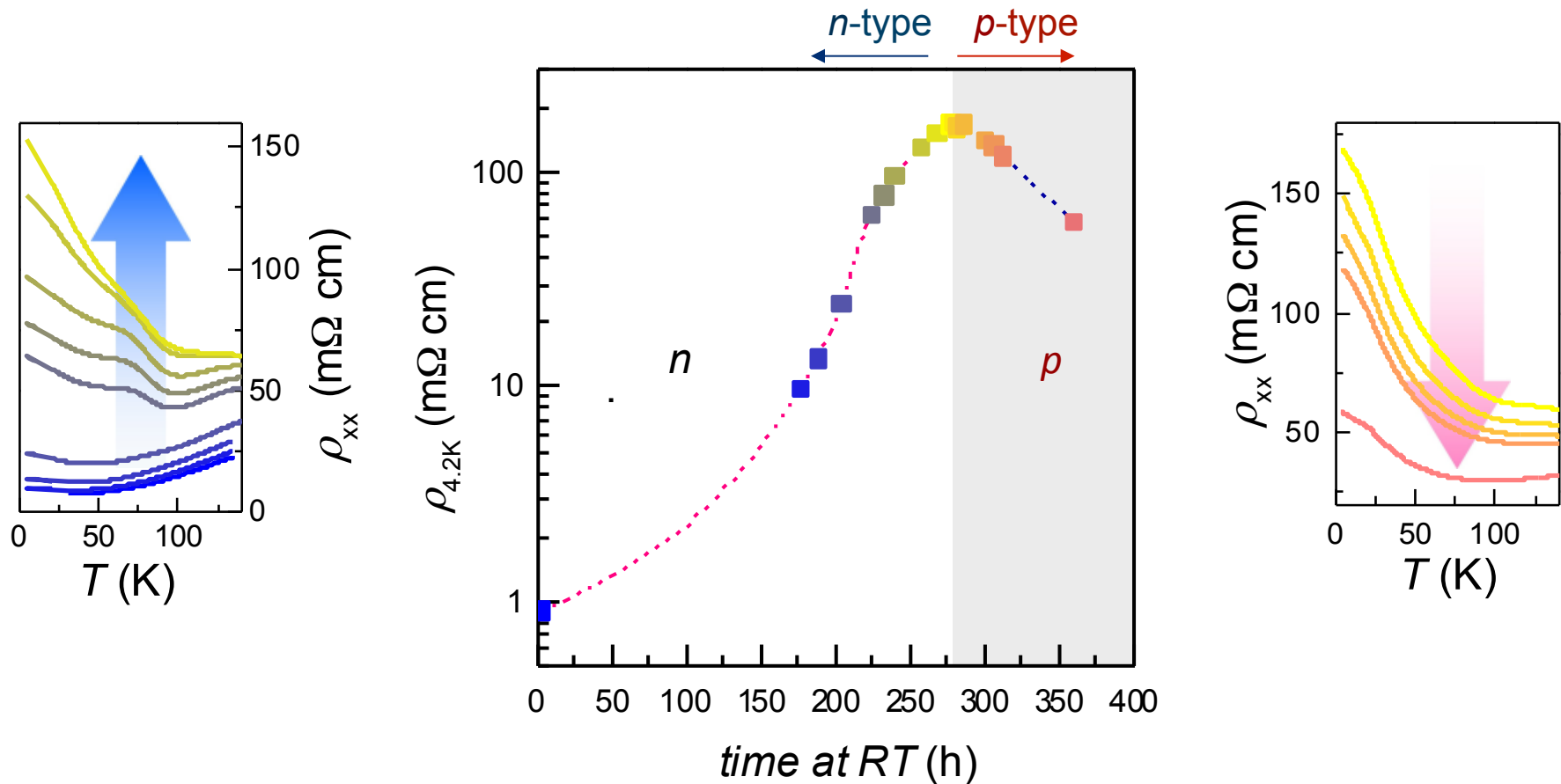


Initial p-type bulk conductivity, concentration from Hall and SdH

Reduction of carrier concentration, until type conversion from p to n

Emergence of surface conduction close to neutrality point. Indexing of Landau levels and analysis of amplitude points to Berry phase of  $\frac{1}{2}$

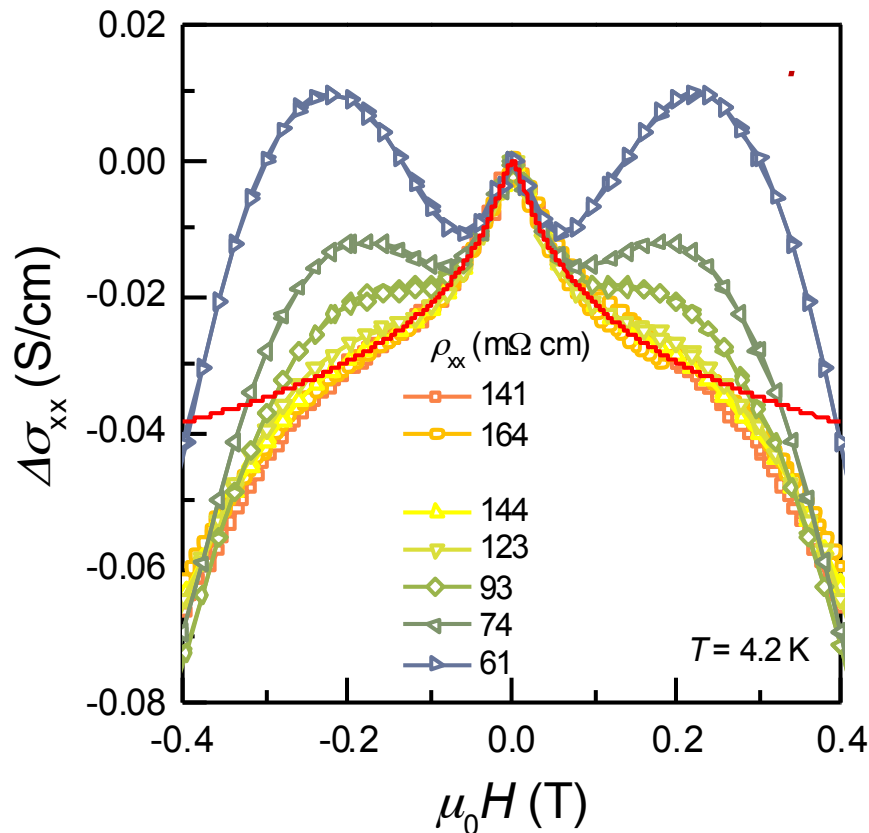
# Room temperature decay of electronic transport properties of irradiated $\text{Bi}_2\text{Te}_3$



*p-type crystal converted to n-type by 2.5 MeV electron irradiation and kept in room temperature*

*Slow evolution of resistivity and carrier concentration: return to p-type*

# Magnetocoductance in the vicinity of CNP



Red continuous curve: fit to Hikami-Larkin-Nagaoka equation

$$\sigma(B) - \sigma(0) \approx C \left( \ln\left(\frac{B_\Phi}{B}\right) - \Psi\left(\frac{1}{2} + \frac{B_\Phi}{B}\right) \right)$$

$$B_\Phi = \frac{\hbar}{4el_\Phi^2} = 37G$$

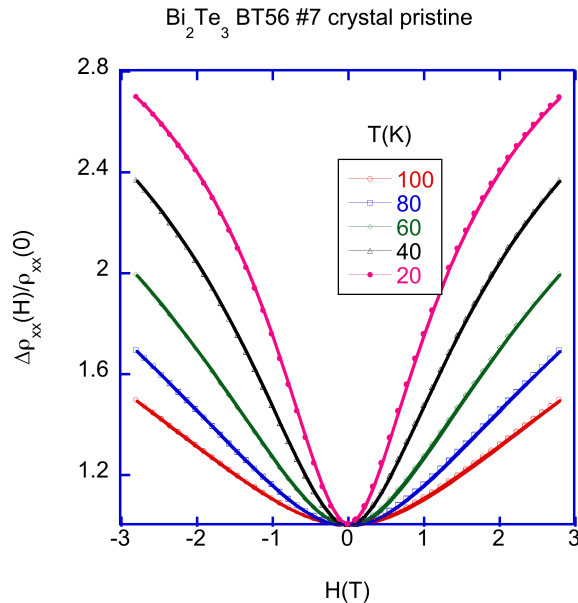
$$l_\Phi = 212nm$$

Magnetocoductivity close to maximum exhibits complex structure with sharp “cusp” invariant with background conductivity and well fitted by weak antilocalization formula  
Bulk and surface conduction channels in parallel

# Distinction between surface and bulk conductivity from magnetoresistance

Bulk orbital magnetoresistance:

$$\frac{\Delta\rho}{\rho} = \left(1 + (\mu B)^2\right)$$



Crosscheck for weak anti-localization on surface channel:  
2D scaling.

Quantum interference:

Hikami-Larkin-Nagaoka equation

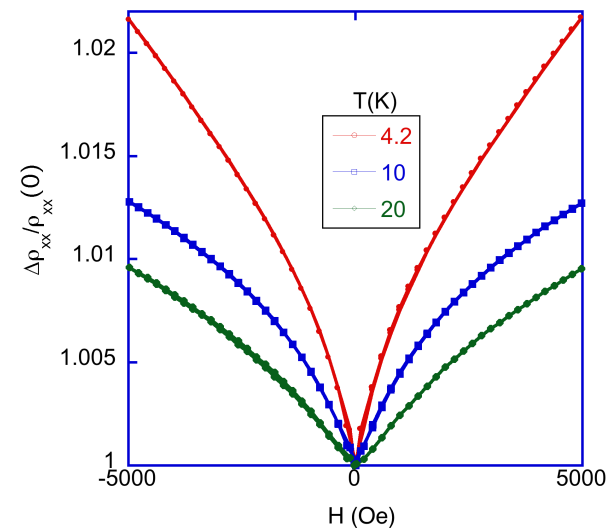
$\alpha = -1$  for weak localization (3D)

$\alpha = \frac{1}{2}$  for weak anti-localization (2D and strong spin-orbit coupling)

$$\sigma(B) - \sigma(0) = \alpha \frac{e^2}{2\pi^2\hbar} \left( \ln\left(\frac{B\phi}{B}\right) - \psi\left(\frac{1}{2} + \frac{B\phi}{B}\right) \right)$$

Bi<sub>2</sub>Se<sub>3</sub>:Ca 44/8 sample #4 irradiated with 2.5 MeV

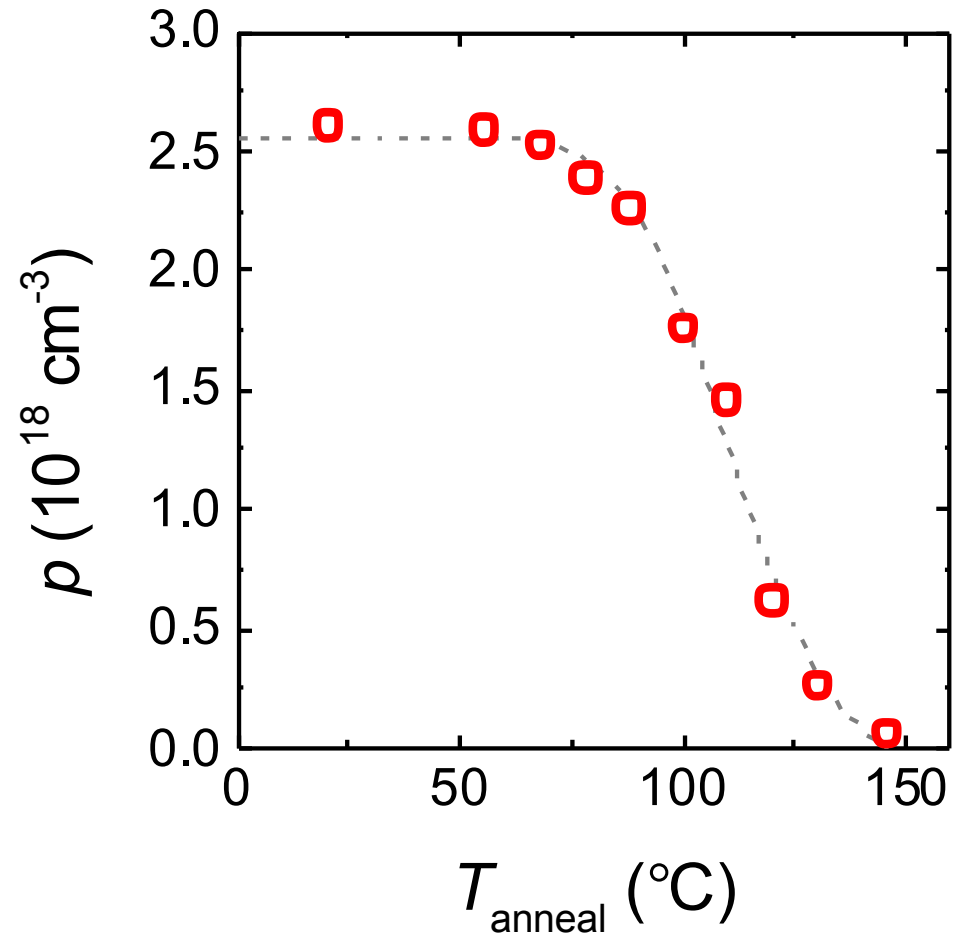
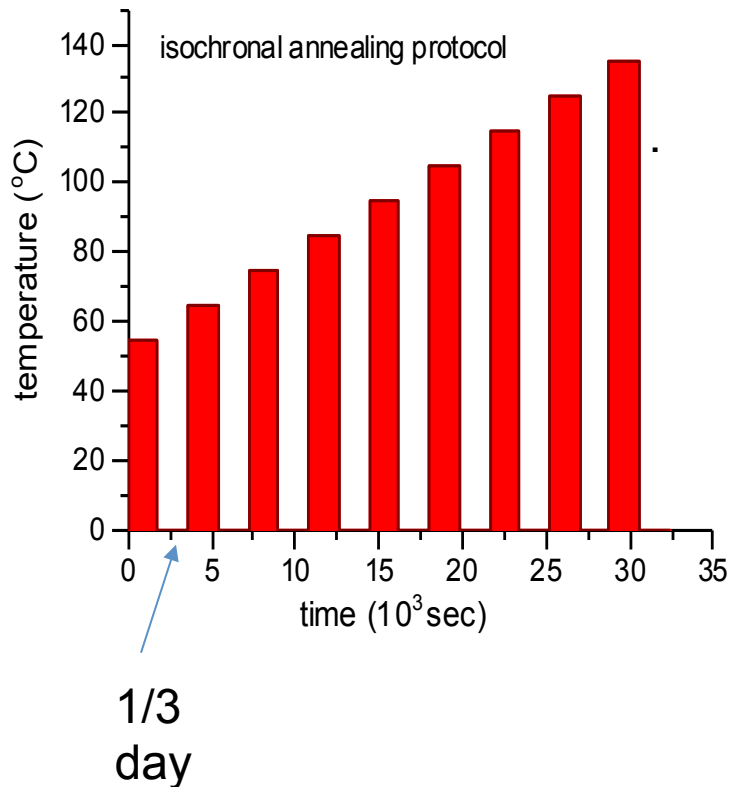
electrons dose 118mC/cm<sup>2</sup> annealed 102°C



# Isochronal annealing of irradiated $\text{Bi}_2\text{Te}_3$

*Irradiation at 20K to the dose below type inversion*

*30 min annealing steps, followed by measurements at 4.2K*



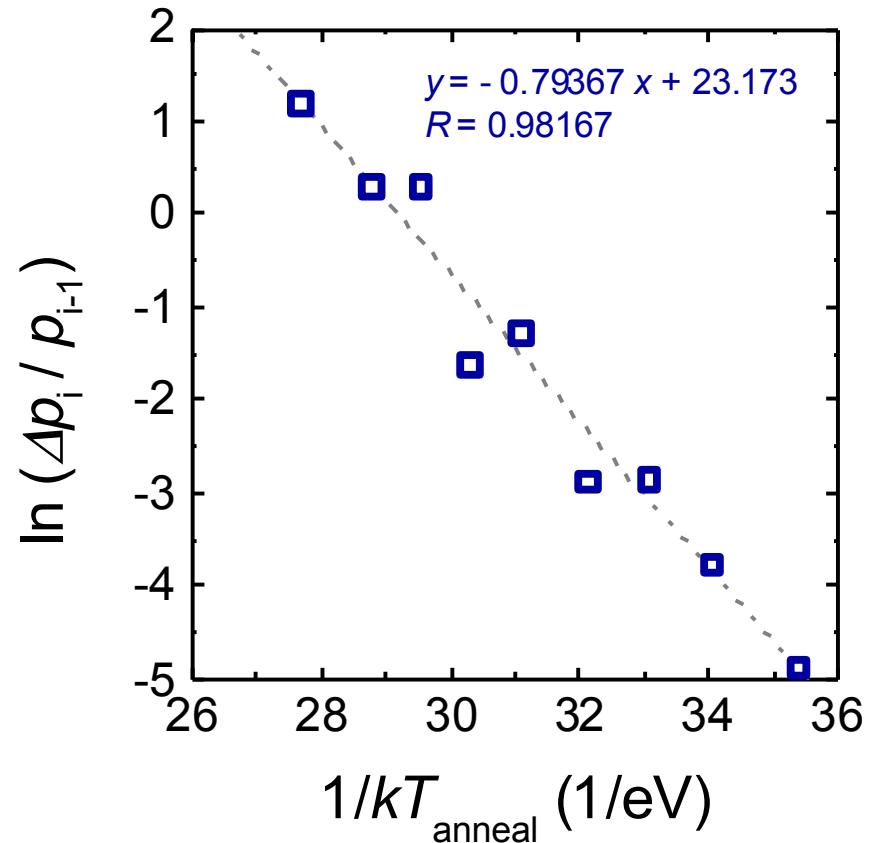
# Isochronal annealing of irradiated $\text{Bi}_2\text{Te}_3$

Standard procedure of analysis of isochronal annealing for process controlled by diffusion equation

$$\frac{\partial p}{\partial t} = -p * e^{-E_b/kT}$$

$$\frac{\Delta p_i}{p_{i-1}} \approx \frac{\partial \ln(p)}{\partial t}$$

$$\ln\left(\frac{\Delta p_i}{p_{i-1}}\right) \approx e^{-E_b/kT}$$

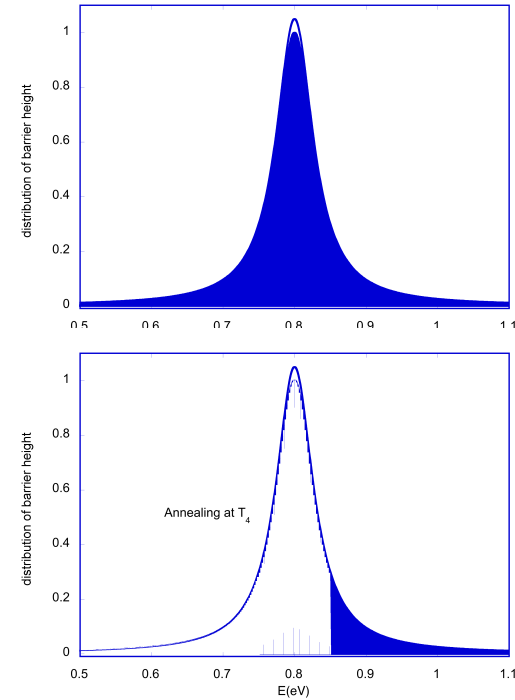
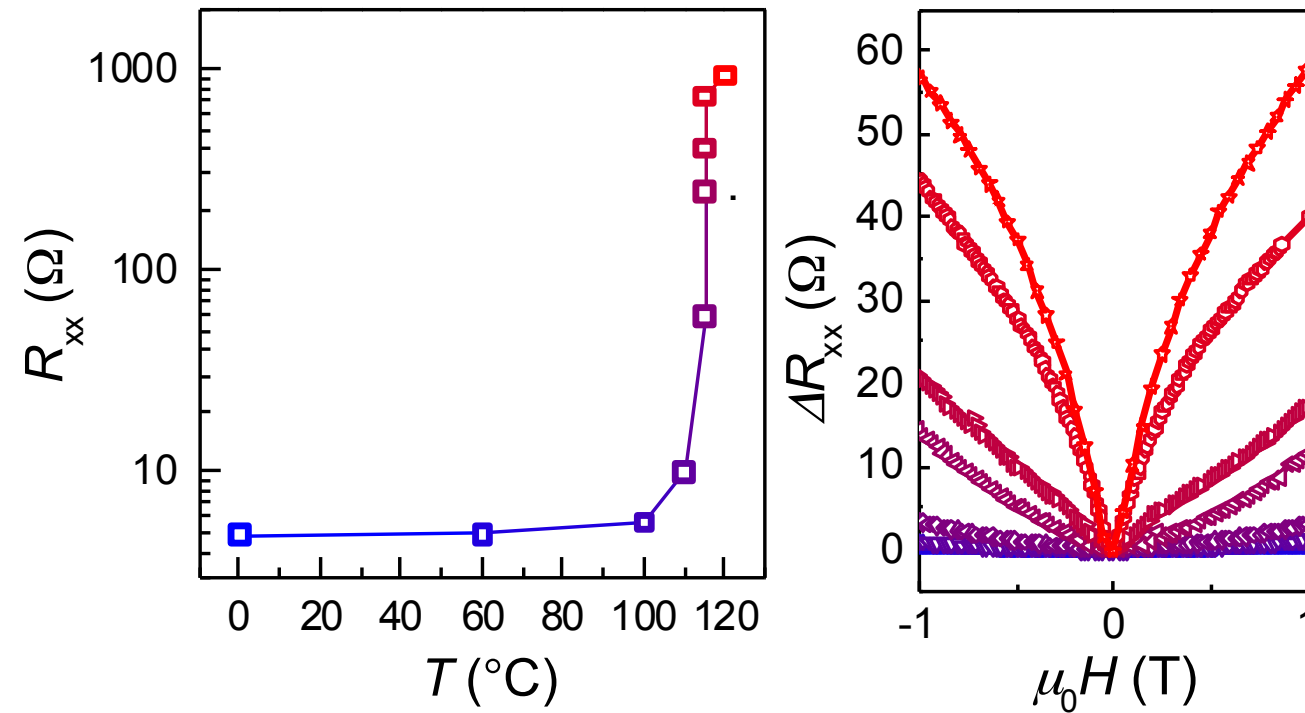


Migration energy  $E_b \sim 0.8\text{eV}$  typical for vacancy migration and compatible with slow decay observed at room temperature.

# Annealing of 2.5 MeV electron irradiated p-type $\text{Bi}_2\text{Te}_3$

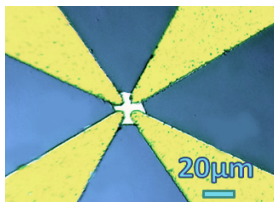
Irradiation to the dose just above charge neutrality point does not guarantee stable high resistance state.

**Alternative approach: high dose irradiation (10x above CNP) followed by annealing.** Possible scenario: formation of more stable defects, divacancies?

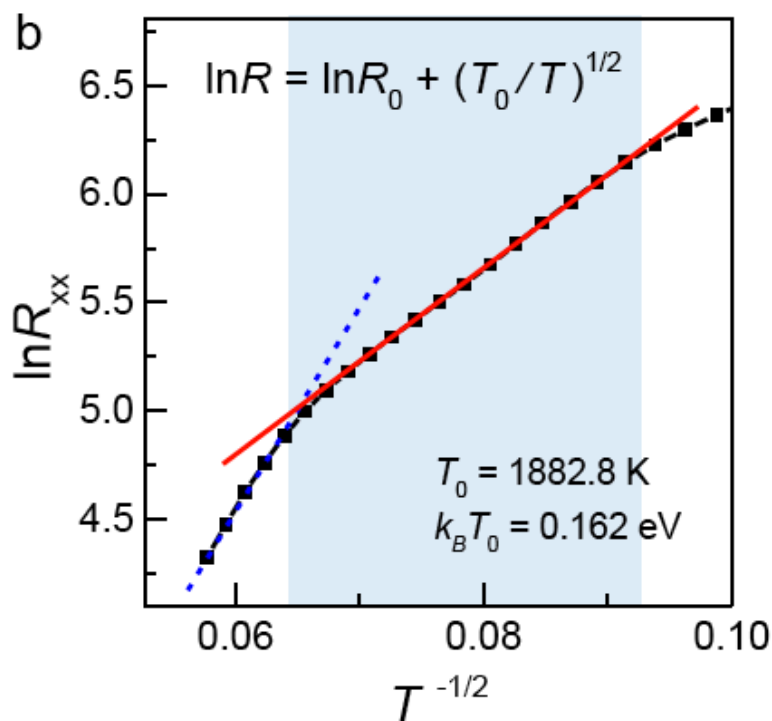
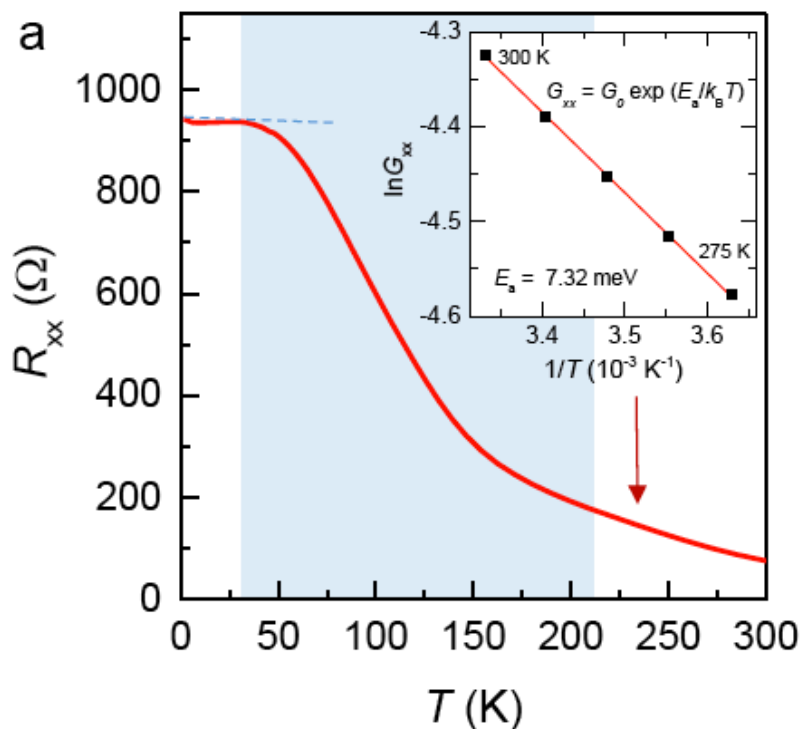


Typical evolution of resistivity and magnetoresistance measured at 4.2K, in the function of annealing temperature of  $\text{Bi}_2\text{Te}_3$  crystal irradiated to  $1\text{C}/\text{cm}^2$

# Electronic transport close to CNP



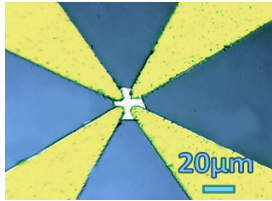
Large bulk sample irradiated, processed (contacted in van der Pauw configuration) and annealed



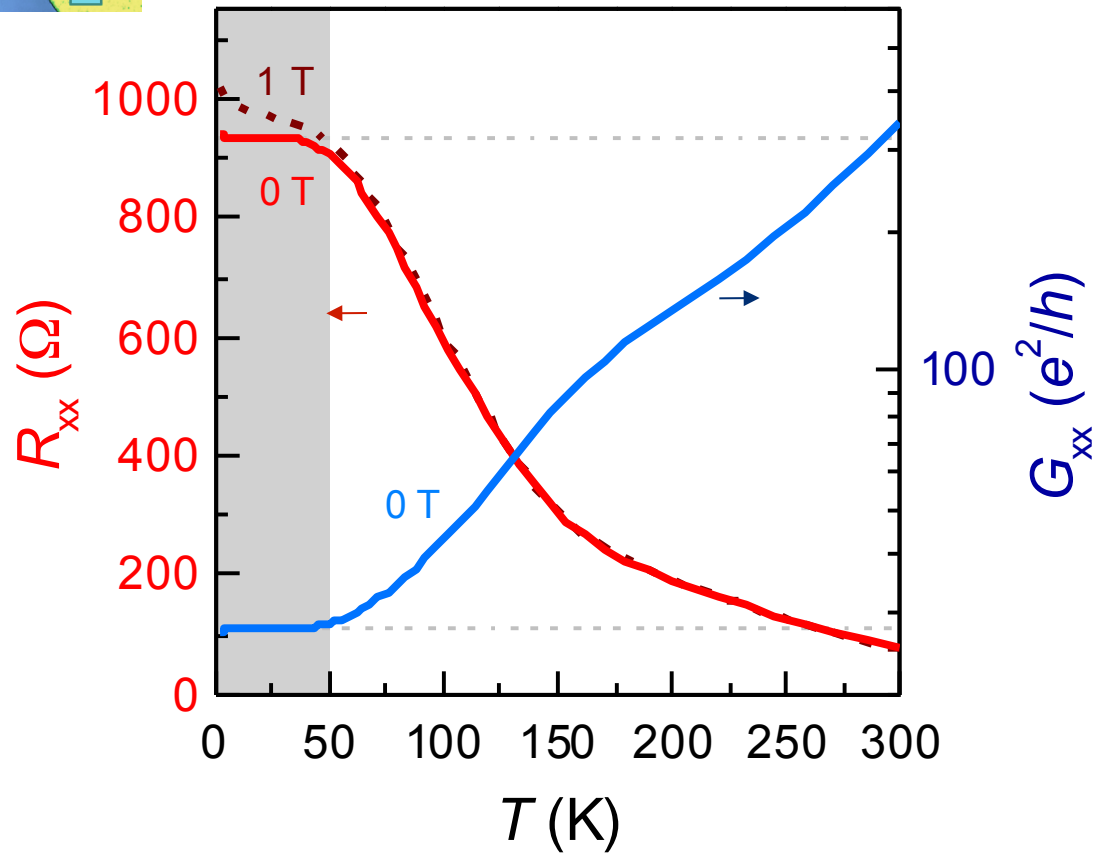
Distinct regions in  $R_{xx}(T)$  curve from thermally activated at high-T to Efros-Shklovskii variable range hopping regime in intermediate T and plateau at low T



# Electronic transport close to CNP

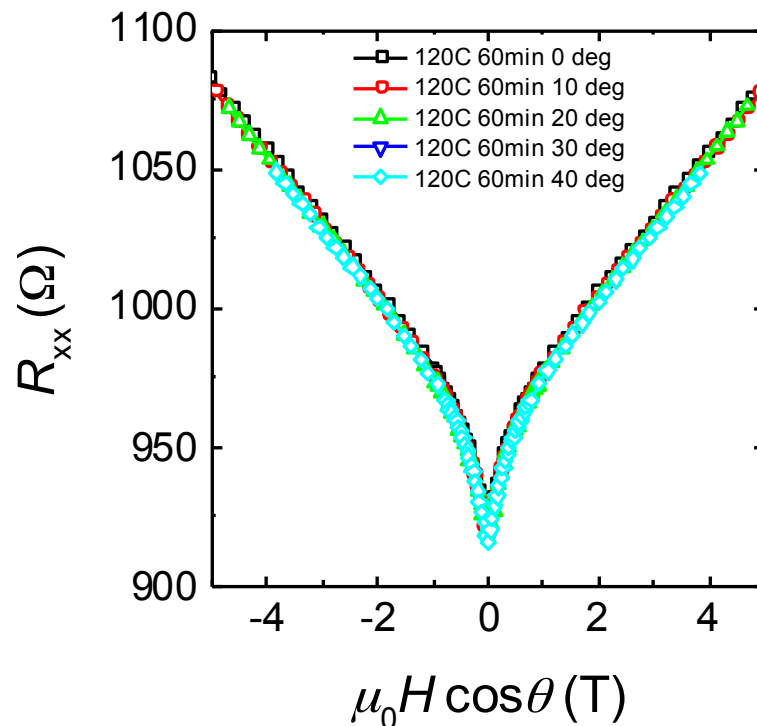
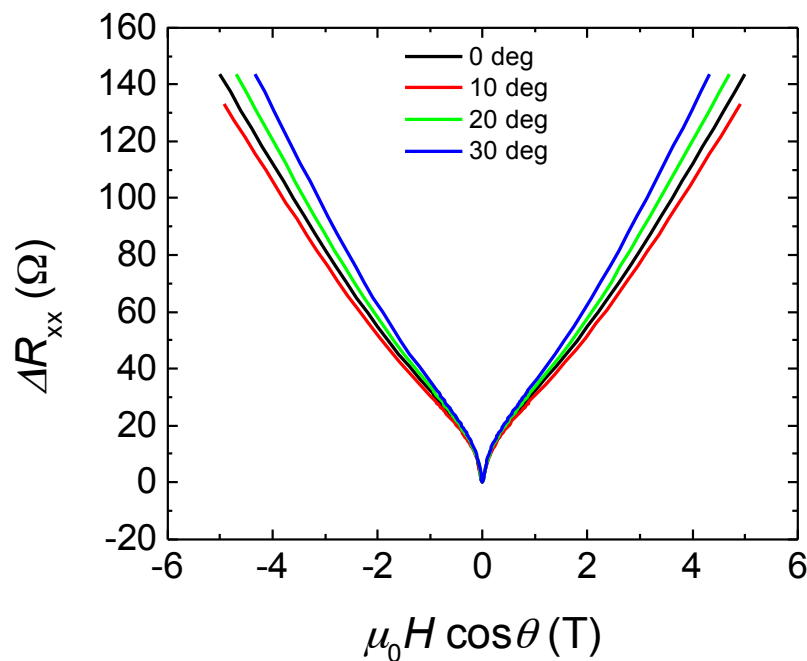


Low temperature plateau disappears in magnetic field. Possible explanation: magnetic field opens gap in Dirac cone



Low temperature conductivity drops to 20  $G_0$  (conductance quanta)

# Angular scaling of magnetoresistance close to CNP



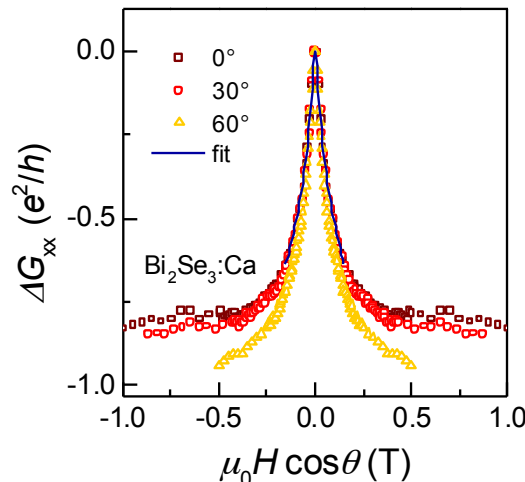
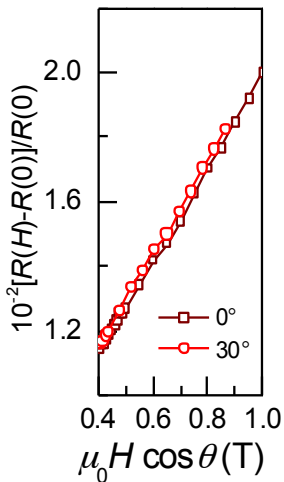
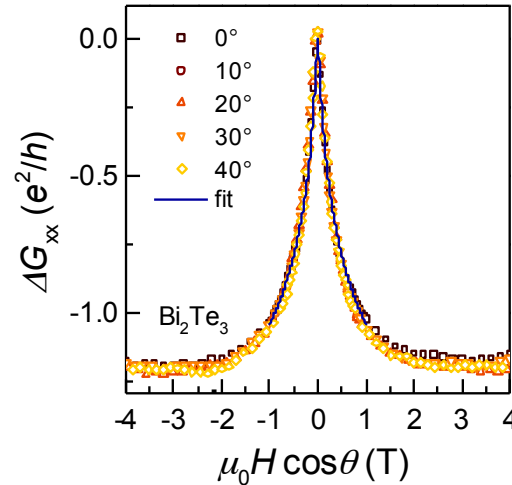
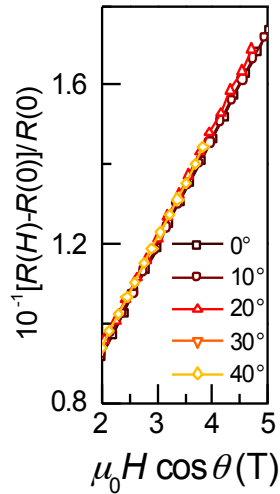
Typical magnetoresistance curves measured at 1.9K on  $\text{Bi}_2\text{Te}_3$  crystals irradiated and annealed to state close to CNP (left) and on CNP (right)

- Outside CNP parabolic MGR scales with B and not  $B\cos(\Theta)$
- At CNP MGR follow 2D scaling in wide field range

Note: high amplitude and linear MGR at high field can not be explained by WAL. Another mechanism is involved, likely Abrikosov “quantum magnetoresistance” (Phys. Rev. B 58, 2788 (1998))

# Analysis of magnetoresistance close to CNP

Experiments on thin exfoliated parts of irradiated and annealed  $\text{Bi}_2\text{Te}_3$  and  $\text{Bi}_2\text{Se}_3$  crystal



Two step procedure:

- (1) Determination of linear MGR at high magnetic field
- (2) Subtraction of this linear MGR
- (3) Fit of remaining part of MGR to HLN formula

$$\Delta G(B) \approx \alpha \frac{e^2}{2\pi^2 \hbar} f\left(\frac{B_\Phi}{B}\right)$$

$$\alpha \approx 1.12$$

$$\text{Bi}_2\text{Te}_3$$

$$\text{Bi}_2\text{Se}_3$$

$$B_\Phi \approx 100\text{G}$$

$$40\text{G}$$

$$l_\Phi \approx 140\text{nm}$$

$$220\text{nm}$$

Remarkably:  $\alpha \approx 1$  means 2 conduction channels (bottom & top)

# Conclusion

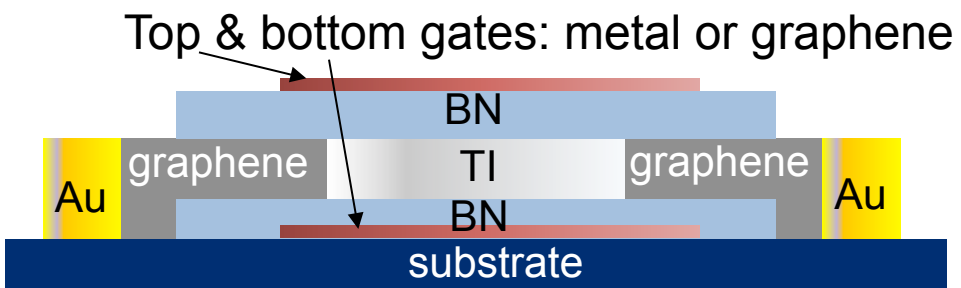
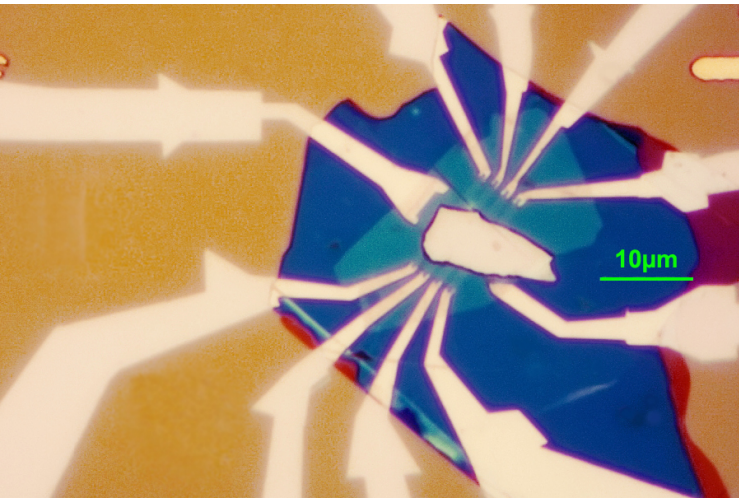
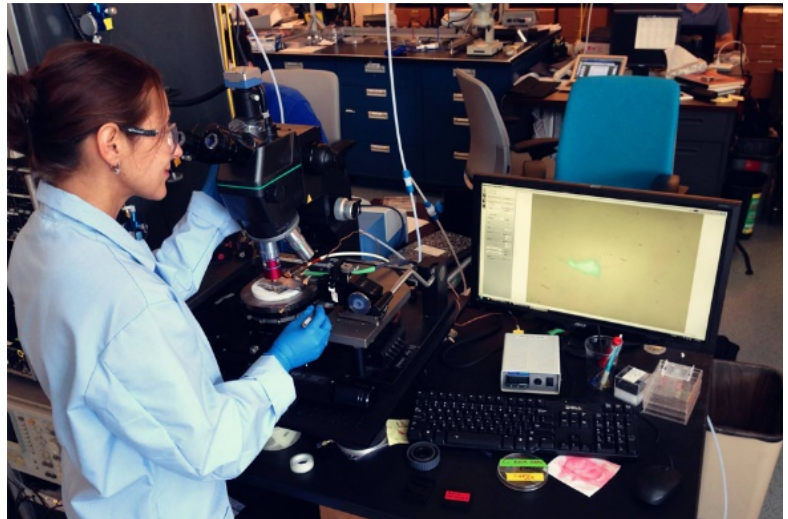
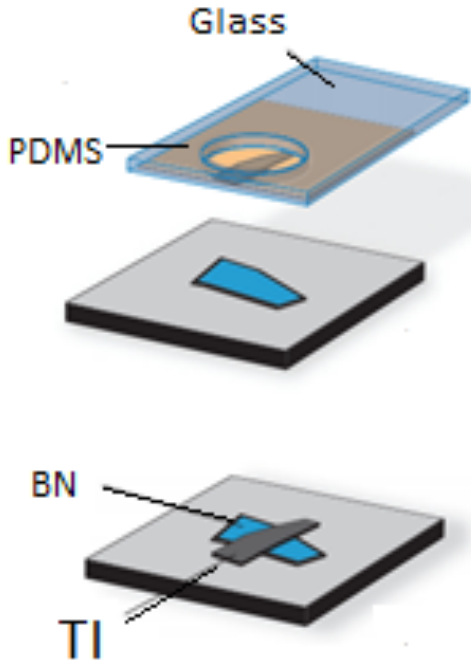
- Doping by energetic particle irradiation of  $\text{Bi}_2\text{Te}_3$  and  $\text{Bi}_2\text{Se}_3$  efficient method to suppress bulk conduction.
- Donor Bi vacancies are main type of defects involved
- Combination of irradiation and annealing lead to material with conduction dominated by surface channel

Zhao, L. M.K et al. *Stable topological insulators achieved using high energy electron beams*. Nat. Commun. 7, 10957 (2016)

# Next steps : Fabricating hybrid gated structures starting from high resistance, irradiated TI's (CUNY)

## General technique

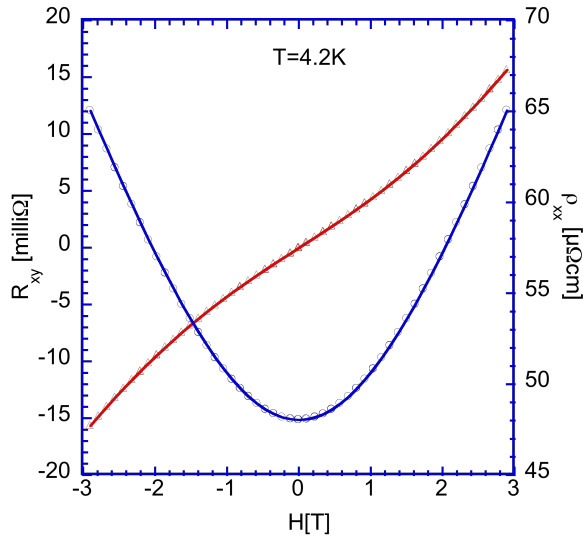
- ✓ Incapsulate TIs (*h*-BN)
- ✓ Use inert environment during fabrication
- ✓ Measure  $R_{xx}$ , Hall, angular dependent  $R$
- ✓ Gate near CNP
- ✓ Heterostructures with magnetic material, SC (in future)



# Next steps : Application to magnetically doped TI's

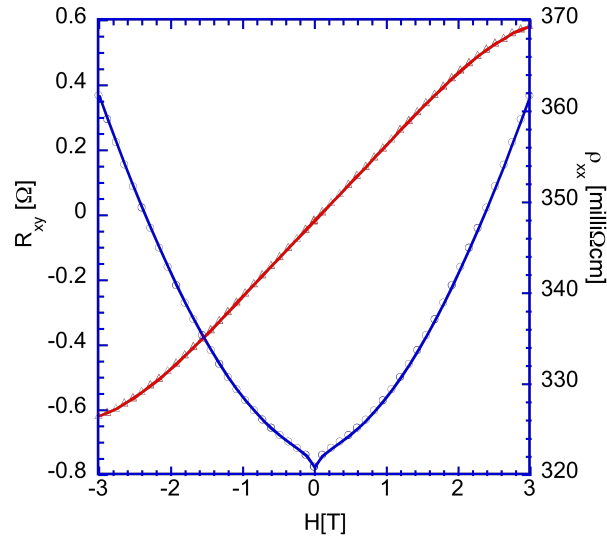
Conductivity type inversion by low temperature electron irradiation  
Ready to step by step annealing to reach CNP

$(\text{Bi}_{1-x}\text{Mn}_x)_2\text{Te}_3$   $x=0.04$  pristine



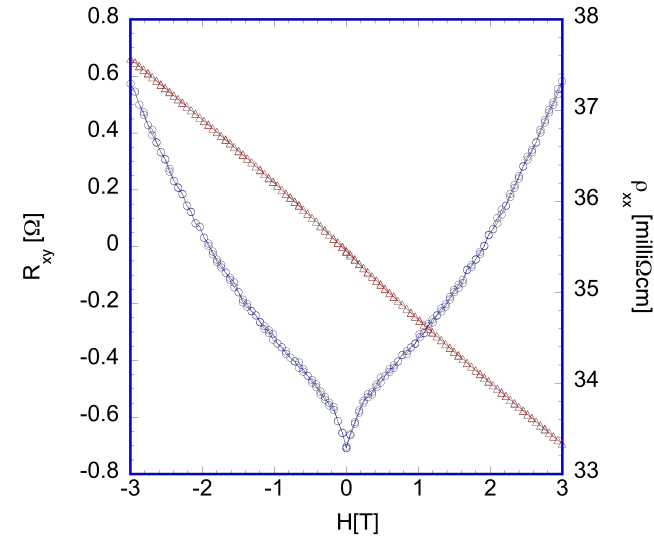
$$\rho = 4.5 \div 7.5 \times 10^{19} \text{ cm}^{-3}$$
$$\mu = 1700 \div 2200 \text{ Vcm/s}^2$$

$(\text{Bi}_{1-x}\text{Mn}_x)_2\text{Te}_3$   $x=0.04$  irradiated  $1.02\text{C/cm}^2$



$$\rho = 1.3 \div 2.5 \times 10^{18} \text{ cm}^{-3}$$
$$\mu = 7 \div 14 \text{ Vcm/s}^2$$

$(\text{Bi}_{1-x}\text{Mn}_x)_2\text{Te}_3$   $x=0.04$  irradiated  $1.9\text{C/cm}^2$



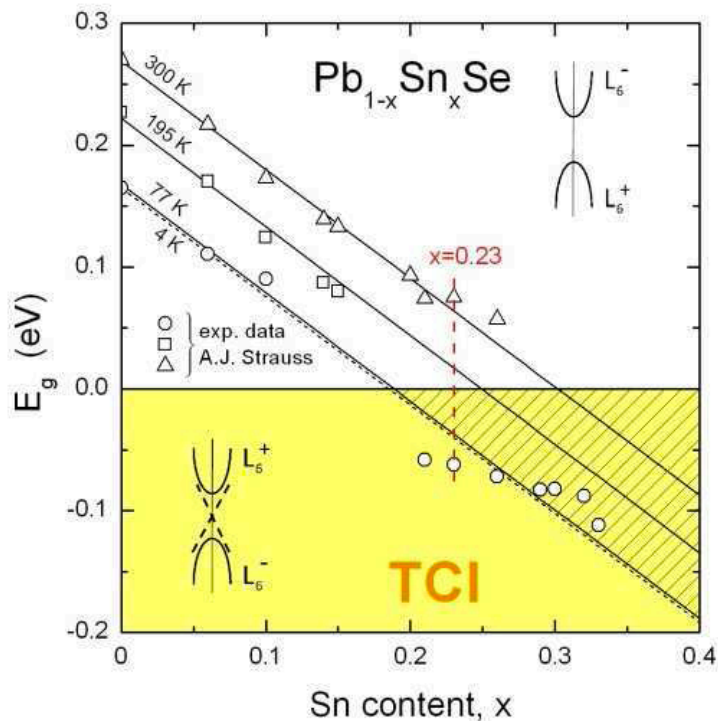
$$n = 1.4 \times 10^{18} \text{ cm}^{-3}$$
$$\mu = 140 \text{ Vcm/s}^2$$

Ready to step by step annealing to reach CNP

# Doping of Crystalline Topological Insulators

$\text{Pb}_{1-x}\text{Sn}_x\text{Se}$  distinct family of TI with crossover from trivial to topological insulator in function of composition.

Crystal symmetry on the origin of topological surface states



The same problem of bulk conduction jeopardizing access to the surface conduction channel.

Can we suppress bulk conduction by irradiation induced doping?

Starting from n-type material we can convert it to p-type.

